

## Analysis of active power control algorithms of variable speed wind generators for power system frequency stabilization

Jakub OSMIC<sup>1,\*</sup>, Mirza KUSLJUGIC<sup>1</sup>, Elvisa BECIROVIC<sup>2</sup>, Daniel TOAL<sup>3</sup>

<sup>1</sup>Faculty of Electrical Engineering, University of Tuzla, Tuzla, Bosnia and Herzegovina

<sup>2</sup>EPC Elektroprivreda B&H d.d. Sarajevo, Department for Development, Sarajevo, Bosnia and Herzegovina

<sup>3</sup>Plassey Technology Park, Department of Electronic and Computer Engineering, University of Limerick, Limerick, Ireland

Received: 24.07.2013

Accepted/Published Online: 02.11.2013

Final Version: 01.01.2016

**Abstract:** A modified control algorithm of a variable speed wind generator (VSWG) for supporting power system frequency stabilization is presented in this paper. A comparison of the performance of this algorithm with active power control algorithms of VSWGs for supporting power system frequency stabilization, as published in the scientific literature, is also presented. A systematic method of analysis of the modified control algorithm is described in detail. It has been shown that by using the modified control algorithm, the VSWG “truly” emulates the inertial response of a conventional steam-generating unit with synchronous generators during the initial/inertial phase of primary frequency control, following loss of active power generation when wind speed is between cut-in (i.e. 4 m/s) and rated speed (i.e. 12 m/s). By the inclusion of a signal proportional to the frequency deviation as a power reference to the torque controller feedback loop of the modified control algorithm, it is ensured that the contribution of the VSWG to frequency stabilization is independent of the initial wind speed. This independence is kept as long as the wind speed is above the cut-in wind speed and slightly below the rated wind speed (i.e. 12 m/s). One of the important features of the modified control algorithm, namely a near-proportional relationship between the initial wind turbine speed and the maximum wind turbine speed variation during the inertial response, has been identified. The results of the analysis provide a solid basis for further research in the area of VSWG contribution to frequency stabilization.

**Key words:** Emulation of inertial response, primary frequency control, frequency stabilization, variable speed wind generator, inertial control algorithms

### 1. Introduction

Due to the increasing penetration levels of variable speed wind generator (VSWG) technology in electrical power generation portfolios, there is a need for these nonsynchronous generators to contribute to grid frequency regulation. Since VSWGs are connected to the network via AC/DC/AC converters, there is no direct coupling between grid frequency deviation and VSWG active power generation. The operation of a VSWG at maximum power point tracing (MPPT) limits its frequency control capability as well. A control algorithm for the VSWG, which will ensure its participation in grid frequency regulation, should ensure extraction of additional electric power from the VSWG during a frequency disturbance.

The steady state of an electric power system (EPS) is characterized by a balance between active power generation and consumption. Following a sudden active power disturbance in an EPS, such as loss of a generating

\*Correspondence: jakub.osmic@untz.ba

unit or a sudden increase in active power load, the rest of the EPS cannot respond instantaneously by increasing the necessary turbine mechanical power to reestablish the power balance. This is due to nonzero time constants of governor and turbine dynamics. As a result, the grid frequency starts to decrease. Immediately after the occurrence of an active power deficit, power balance is first established from electromagnetic energy accumulated in the synchronous machines. Then the provided EPS transient stability is maintained, and in the so-called inertial phase of rotating machine frequency response, generator kinetic energy is converted to active power and delivered to the rest of the system to maintain active power balance. This process results in generator rotational speed and frequency decline. The inertial phase lasts no more than several seconds. In the inertial phase, due to the action of the speed regulator (droop control), the prime mover also starts delivering additional mechanical power to the generator. The provided frequency stability is maintained, and the inertial response and droop control action combined result in recovery of frequency/machine rotation speed and kinetic energy. Finally, after typically 30 s, the frequency of the system stabilizes at the new steady-state value. The permitted interval of the grid frequency variation is quite short, so the system of turbine mechanical power regulation must be fast enough to prevent frequency deviation below the minimum allowed level.

The most frequently used types of modern large power wind generators are VSWGs, such as double fed induction generators (DFIGs) and fully rated converter wind turbines (FRCWTs) [1–4]. Since DFIGs and FRCWTs use fast electronic converters (AC/DC/AC) and operate at MPPT, there is no (or very little) direct coupling between grid frequency deviation and their active power generation. Operation at MPPT results in VSWGs having no “spinning reserve” that could be used to support frequency regulation after disturbance. It is, therefore, necessary to modify VSWG active power control algorithms to support grid frequency regulation. DFIG and FRCWT frequency regulation capabilities have been a focus of interest in the scientific community in recent years [5–14]. As a result, a number of papers have been published dealing with different control algorithms for use with VSWGs, designed to provide a contribution to primary frequency control [2,4,15]. These control algorithms can be classified into inertial control, droop control, deloading control, or combinations of these [5–7,9,12,14]. All the above-mentioned approaches pertain to individual VSWG control. Control algorithms for control coordination at the wind farm level or the EPS as a whole, such as in [10,13], are also proposed.

The inertial control approach enables transformation of a fraction of VSWG kinetic energy into electrical power, which is “instantaneously” delivered to the EPS by the (fast) electronic power converter. The time constant of the electronic converter is of the order of milliseconds. The transformation of kinetic energy to electric power causes a VSWG speed decrease, which must be limited in order to prevent the turbine speed from reaching its minimum permitted level. In addition, since VSWGs normally operate at MPPT, wind generator speed should be recovered to this optimum value after the frequency stabilization. Since VSWGs normally operate without spinning reserve, speed recovery is performed by the VSWG delivering less active electric power than optimum (maximum available). This ensures that the speed of a VSWG recovers to its optimum value (for the constant wind speed case, to the value before the frequency transient).

The main challenge in VSWG inertial (and droop) control is that of “shaping” the response of the active power delivered to the rest of the EPS as well as the speed response of the VSWG after the frequency disturbance. A number of different inertial and droop controllers or their combinations have been proposed, as presented in [5–7,9,12–14]. The main idea, presented in these approaches, is to add a new control signal  $C_{ad}$  to the existing torque control loop, before or after the torque controller, which will force the VSWG to emulate the inertial response or the inertial response plus droop control of the conventional generators. Then this combined signal appears as the reference torque input  $C_{ref}$  to the electronic converter, such as in [6], or as the reference

active power input  $P_{ref}$ , as in [9]. These approaches are illustrated in Figure 1. The symbols used in this figure have the following meaning:  $P_e$  represents measured active power of wind unit,  $\omega$  represents grid frequency,  $\Delta\omega$  represents grid frequency deviation,  $\omega_t$  is VSWG speed,  $\Delta\omega_t$  is VSWG speed deviation,  $C_{set}$  is the control signal from the PI controller, and  $C_{ad}$  is an additional control signal for inertia and droop emulation. In the referred research for inertia emulation, the so-called washout filter is used for inertial signal zeroing at network frequency steady state as well as for grid frequency (or frequency deviation) signal filtering. A washout filter, in fact, performs filtered derivation of the grid frequency (or frequency deviation) signal. In some papers, an additional compensator block is used to create phase compensation of the signal leaving the washout filter [5]. If the signal  $C_{ad}$  is added after the torque PI controller, then the torque control loop considers this signal as the disturbance signal. In this case, it is not necessary to derivate the grid frequency signal, since the integral part of the torque controller makes this signal of no effect at steady state, even if the steady state value of  $\Delta\omega$  is different from zero. The droop part of the additional signal  $C_{ad}$  in Figure 1 is used to emulate the droop behavior of a conventional regulator in primary frequency control. Figure 2 shows a schematic diagram of the active power and pitch angle controllers for a DFIG, as presented in [14]. An almost identical schematic diagram can be applied to FRCWTs. With reference to Figure 2, in order to emulate primary frequency regulation, the torque signal  $\Delta T_{set}$ , proportional to deviation of grid frequency  $\Delta\omega$ , is combined with the signal from the torque controller, in which way the modification of the torque set point  $T_{set}$  is performed. An important conclusion in [14] is that the inertial support from the DFIG is dependent on the kinetic energy stored in the turbine blades, and, consequently, frequency support is dependent on the captured mechanical power of the wind turbine. In addition, in [14] it is stated that the inertial response of DFIG is dependent on the initial operating conditions; accordingly, it is dependent on the initial rotational speed of the DFIG. In this paper, it is shown that by using a modified control algorithm with a different point of insertion of the additional signal  $C_{ad}$  that is proportional to network frequency deviation, as shown in Figure 3, it is possible to achieve a result where the inertial support is independent of the initial operating conditions, as long as the wind speed is between the cut-in wind speed (4 m/s) and the rated wind speed (12 m/s).

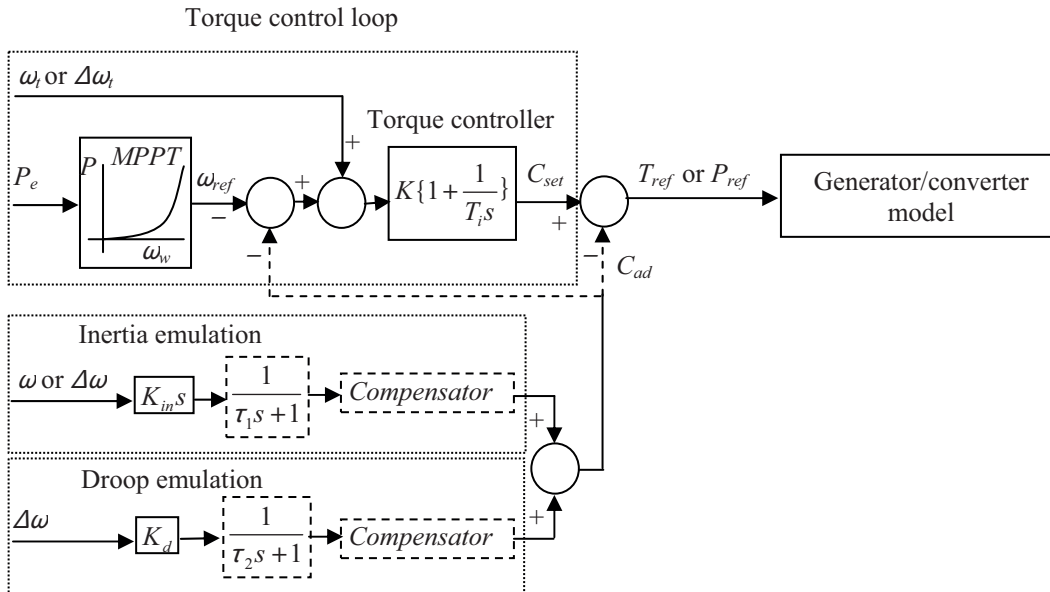
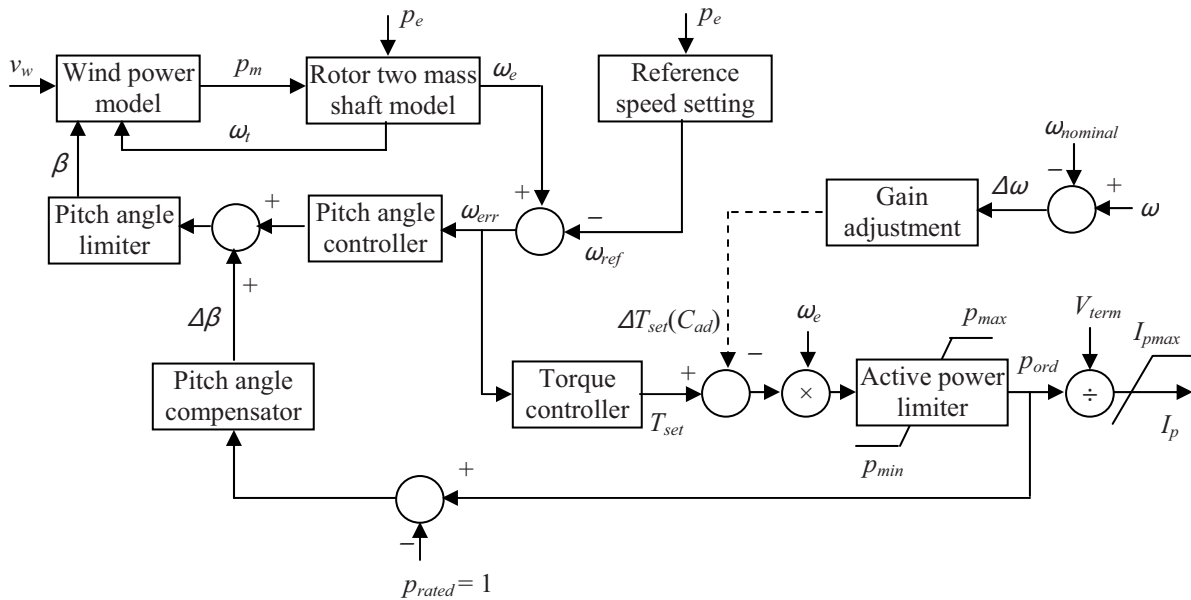


Figure 1. Control loops for wind unit active power control.



**Figure 2.** Schematic diagram showing active power and pitch angle controllers of DFIG (adopted from [14]).

## 2. Analysis of VSWG control system with an added inertial support controller

In Figure 3, a detailed block diagram of the modified control algorithm of the active power-torque and pitch angle control of VSWG is presented. The main parts of the modified control algorithm are adopted from [3,8,16–19]. Based on the recommendations of [19], a VSWG wind farm could be represented by the equivalent one-mass wind turbine model. Hence, the modified control algorithm can be used for simulation of the frequency response of a wind farm. In Figure 3, point *A* is the point of insertion of the inertial support signal. It can be seen that the inertial support signal is added after the block of multiplication of the reference torque signal with the actual turbine speed  $\omega_t$ . This point of insertion of the inertial support signal is used in [20], but without considering the impact of the selection of the point of insertion on the independence of VSWG inertial support from the initial wind speed. Moreover, in [20], a different support algorithm for frequency stabilization from the support algorithm used in this paper is proposed. In Figure 3, the symbol *G* represents the transfer function of the inertial support controller, which in this paper is the transfer function of the proportional controller. For simplicity of analysis, it is assumed that the turbine speed equals the generator speed  $\omega_e$ .

The analysis of VSWG control for supporting grid frequency depends on the regions of wind speed in which the VSWG operates. The normal VSWG control strategy, which is also used in this paper, is described as follows. For a wind speed below cut-in speed of 4 m/s, the VSWG is turned off; for a wind speed between cut-in speed and rated speed of 12 m/s at the stationary state, i.e. when wind speed is constant, the VSWG operates at MPPT with minimum pitch angle of  $\beta = 0^\circ$ . In this way it is ensured that the extracted mechanical power is maximal. Since extracted mechanical power, and consequently power injected to the system, is a function of the third power of wind speed, it follows that only at a wind speed that is close to the rated speed (for example, speed over 11.5 m/s) does the injected power, due to the inertial support, approach  $P_{rated}$ . For a wind speed that is slightly below the rated wind speed (for example, below 11.5 m/s) during the VSWG inertial support phase, the injected power usually does not reach  $P_{rated}$ . For wind speed above the cut-out wind speed the turbine stalls. In the region between cut-in and rated wind speed, the control strategy is to

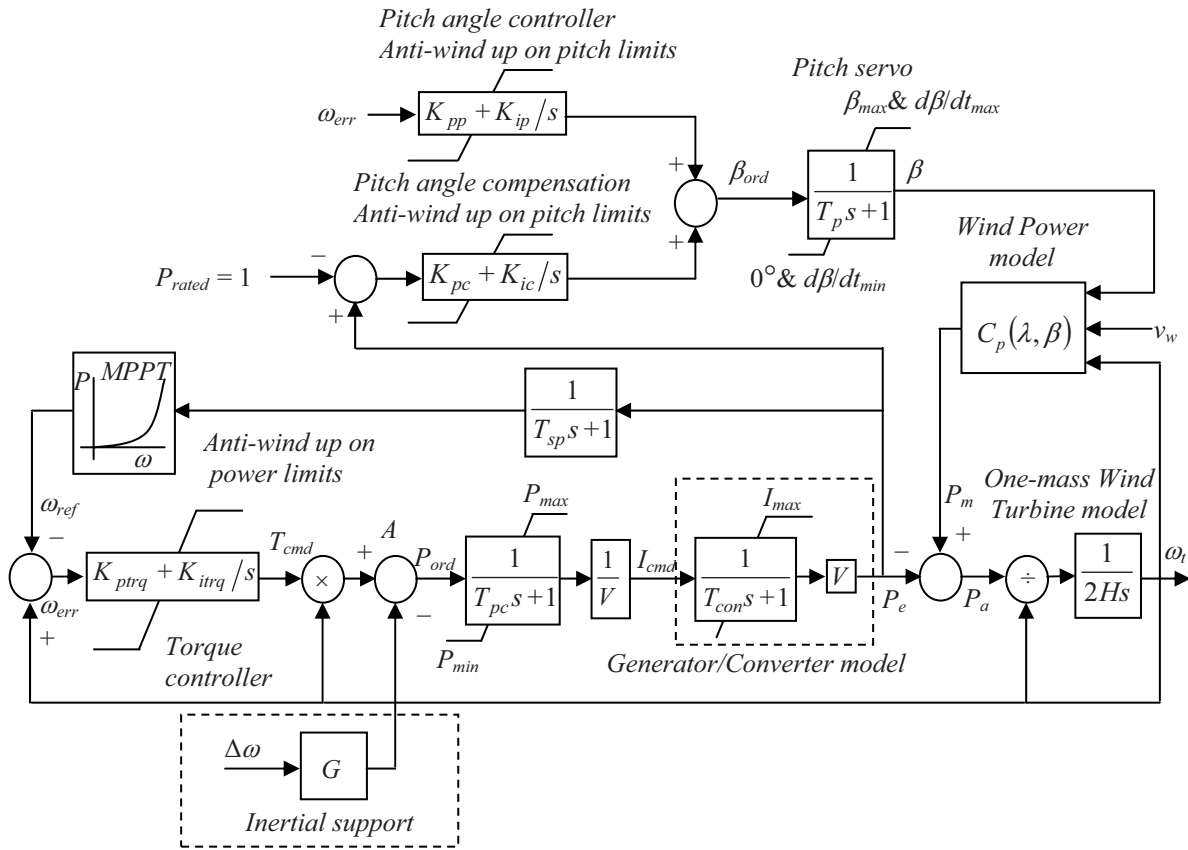


Figure 3. Block diagram of the modified control system of VSWG.

extract the maximum available mechanical power from the wind. This can be achieved when the pitch angle is at zero and when the turbine speed is at the optimal level. In this region, only the pitch controller and the torque controller can produce positive outputs, since electrical power is mostly below rated power and the pitch controller output, due to anti-wind-up at the lower limit, is kept at the lower limit. Therefore, the sum signal from the pitch controller and pitch compensator, which is the input signal into the pitch servo block, is zero or negative. Due to the lower zero-level saturation of the pitch servo block, the pitch angle is kept at  $0^\circ$ . In the region of wind speed between the rated wind speed and the cut-off speed, the PI type pitch controller, PI type pitch compensator, and PI type torque controller ensure that electrical power and turbine speed are kept at the rated level. Integral (I) parts of these controllers ensure that pitch angle and turbine speed, at the stationary state, are kept at the desired level, while the proportional (P) parts of these controllers ensure better transient behavior of the wind turbine control system.

The parameters of the controller structure shown in Figure 3 are given in Table 1. The parameters of the controller are identical to those recommended in [19], except that the  $K_{itrq}$  parameter of the torque controller is slightly changed according to the considerations given in this section. It should be mentioned that in the simulation it is allowed that for short periods of time the converter can deliver power  $P_{max}$ , which is 10% above  $P_{rated}$ .

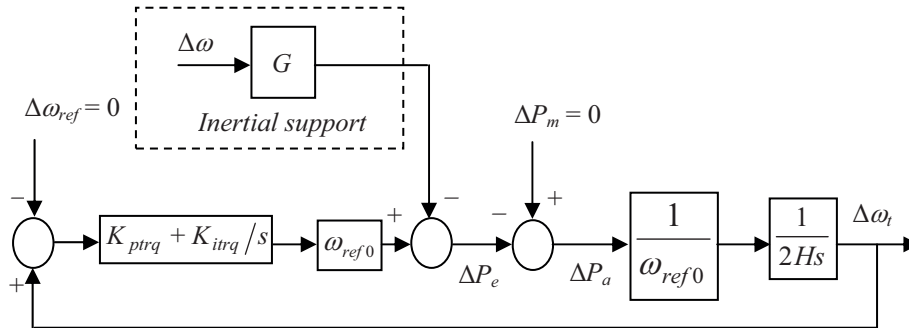
In the following part of the paper, an analysis of the most common situation, when wind speed is between cut-in and rated values, is presented. This analysis covers the situation of loss of a generating unit or a sudden increase of system load.

**Table 1.** Parameters of VSWG control system (see Figure 3).

$K_{pp}$	$K_{ip}$	$K_{pc}$	$K_{ic}$	$T_p$ (s)	$\beta_{max}$ (deg)	$T_{sp}$ (s)	$T_{pc}$ (s)
150	25	3	30	0.3	27	60	0.05
$K_{ptrq}$	$K_{itrq}$	$V$ (pu)	$T_{con}$ (s)	$H$ (s)	$P_{rated}$ (pu)	$I_{max}$ (pu)	$G$
3	0.27	1	0.02	4.18	1	1.1	21.7

The block diagram in Figure 3 is nonlinear, which complicates its analysis and synthesis. A method for linearization of the block diagram, shown in Figure 3, is presented below.

A typical value of time constant  $T_{con}$  is 0.02 s [19]. A typical value of time constant  $T_{pc}$  is 0.05 s. In comparison to the time duration of the frequency transient process, these time constants can be neglected. In order to obtain a linear model, limiters are neglected as well. This is a reasonable assumption, since for a wind speed from 4 m/s to almost 12 m/s these limits should not be activated. A typical value of time constant  $T_{sp}$  is 60 s (such as in [19]). Accordingly, during the frequency transient process the reference rotational speed  $\omega_{ref}$  shows very small changes. Therefore, in the linear case,  $\omega_{ref}$  can be regarded as constant during the entire frequency transient process. Since the VSWG operates at MPPT in a predisturbance steady state, VSWG speed is optimal. In the vicinity of the optimal VSWG speed, the diagram's tip speed ratio ( $\lambda$ ) vs. captured mechanical power ( $P_m$ ) is somewhat flat in comparison to other regions of this diagram. Since the frequency transient process is relatively short, it is expected that the wind speed will not change considerably. Consequently, and taking into account that the pitch angle equals zero, the captured mechanical power of a VSWG can be regarded as constant during the frequency transient process. If a large variation in VSWG speed is not expected, then, for analysis and synthesis purposes, the VSWG speed signal ( $\omega_t$ ) entering the block of multiplication and division can be regarded as constant; that is,  $\omega_t = \omega_{ref0} = const.$ , where  $\omega_{ref0}$  represents the optimal VSWG rotational speed before the frequency disturbance. If the variations of signals around equilibrium points are considered, then the linear model of the system, presented in Figure 4, could be developed. The block diagram from Figure 4 also includes an additional control signal used for frequency stabilization contribution. A new control signal is added after the multiplication of the signal, leaving the torque controller by the actual wind speed. Figure 4 shows that the electrical power injected by the VSWG into the EPS after the frequency disturbance is given by:


**Figure 4.** Linear control structure of the modified VSWG control algorithm with added inertial frequency support.

$$\Delta P_e = -\Delta P_a. \quad (1)$$

The transfer function from  $\Delta\omega$  to  $\Delta P_e$  is given as:

$$\frac{\Delta P_e}{\Delta\omega} = -\frac{G}{\Delta}, \quad (2)$$

where  $\Delta = (1 - \text{loop\_gain})$  represents the characteristic function of the system, which is given by:

$$\Delta = 1 + \left( K_{ptrq} + \frac{K_{itrq}}{s} \right) \omega_{ref0} \frac{1}{\omega_{ref0}} \frac{1}{2Hs} = \frac{2Hs^2 + K_{ptrq}s + K_{itrq}}{2Hs^2}. \quad (3)$$

Substituting Eq. (3) into Eq. (2) gives:

$$\frac{\Delta P_e}{\Delta \omega} = -\frac{\Delta P_a}{\Delta \omega} = -\frac{G}{\Delta} = -\frac{s^2 G}{s^2 + \frac{K_{ptrq}}{2H}s + \frac{K_{itrq}}{2H}}. \quad (4)$$

From Eq. (4) it could be concluded that the VSWG electrical power injected into the EPS during a grid frequency transient process does not depend on initial turbine speed. Consequently, it does not depend on initial wind speed value, i.e. initial mechanical power. This is true regardless of  $G$  being a proportional control law or a more sophisticated control law. Due to the presented assumptions, this is a simplification of the real situation. However, as will be shown with the simulation in Section 3, the former conclusion is valid even in a realistic situation.

The poles of the transfer function of Eq. (4) are:

$$\Delta_{1/2} = -\frac{K_{ptrq}}{4H} \pm \frac{1}{2} \sqrt{\left( \frac{K_{ptrq}}{2H} \right)^2 - \frac{2K_{itrq}}{H}}. \quad (5)$$

If a requirement of the VSWG torque control system, shown in Figure 4, is that the fastest response without overshoot to a step of  $\Delta \omega_{ref}$  be achieved, then parameters  $K_{ptrq}$  and  $K_{itrq}$  of the torque controller should be chosen so that the poles of Eq. (5) are real, negative, and equal (the transfer function of Eq. (4) must have a double negative pole). The pole of the transfer function of Eq. (4) is a double pole and is equal to:

$$\Delta_{1/2} = -\frac{K_{ptrq}}{4H}, \quad (6)$$

if the following equation is valid:

$$K_{itrq} = \frac{H}{2} \cdot \left( \frac{K_{ptrq}}{2H} \right)^2 = \frac{K_{ptrq}^2}{8H}. \quad (7)$$

Due to the integral part of the torque controller, the VSWG speed is equal to the reference speed at steady state. From Eq. (4) it follows that:

$$\Delta P_e = -\frac{s^2 G}{s^2 + \frac{K_{ptrq}}{2H}s + \frac{K_{itrq}}{2H}} \Delta \omega = -\frac{s^2 G}{\left( s + \frac{K_{ptrq}}{4H} \right)^2} \Delta \omega. \quad (8)$$

In addition, from Figure 4:

$$\Delta \omega_t = \frac{1}{2H\omega_{ref0}} \cdot \frac{sG}{s^2 + \frac{K_{ptrq}}{2H}s + \frac{K_{itrq}}{2H}} \Delta \omega. \quad (9)$$

From Eq. (9) it follows that there is an inverse proportionality between the VSWG speed deviation  $\Delta \omega_t$  and the initial turbine speed  $\omega_{ref0}$ . This fact will again be addressed in Section 3. From Eq. (8) it follows that  $\Delta P_e$  diminishes in the steady state due to the existence of term  $s^2$  in the numerator of the transfer function.

In addition,  $\Delta\omega_t$  also reaches zero as time passes, if there is no pole of  $G$  at the origin of the  $s$  plane (that is, if there is no  $s$  in the denominator of  $G$ ). This is due to the existence of  $s$  in the numerator of the expression at the right hand side of Eq. (9). This way it is ensured that the speed and electrical power of the VSWG at steady state are restored to the values from before the frequency disturbance. From the above considerations we can also conclude that, in order to achieve the specified goals, the existence of the term  $s$  (ideal derivation) in the numerator of  $G$  is unnecessary. This is qualitatively a new observation in comparison to most published papers, since they presented the transfer function of the controller, including the  $s$  in the numerator, such as in [6,7,9,11,13]. In [14] it was noted that being an improper transfer function, the derivate function can only be approximated. Furthermore, the derivate block amplifies noise signals. In [14], proportional control is used for the inertial support controller. The same type of controller has been used in the analysis presented in this paper, but with a different point of insertion of the inertial support signal, as has already been mentioned.

### 3. Simulation results

The nine-bus system presented in [21], with an added bus (no. 10) to which a VSWG is connected, as shown in Figure 5, is used as a simulation example in the analysis. The VSWG farm consists of 40 units, each with a rated power of 2.5 MW. The transmission line between bus 7 and bus 10 is exactly the same as the transmission line between buses 7 and 8. In the analysis, it is assumed that during simulations the VSWG produces only active power. Since system load is assumed to be constant, the initial generation of active power from steam generator  $G2$  is reduced by the amount of the VSWG active power generation  $P_{VSWG0}$ , which depends on initial wind speed. The network data and initial steady state data necessary for power flow calculations are presented in Figure 5. Generator data and turbine data, adopted from [21], are given in Table 2. MATLAB Function Block: Hydraulic Turbine and Governor Data are given in Table 3. Table 4 shows MATLAB Function Block: Steam Turbine Data and Governor Data.

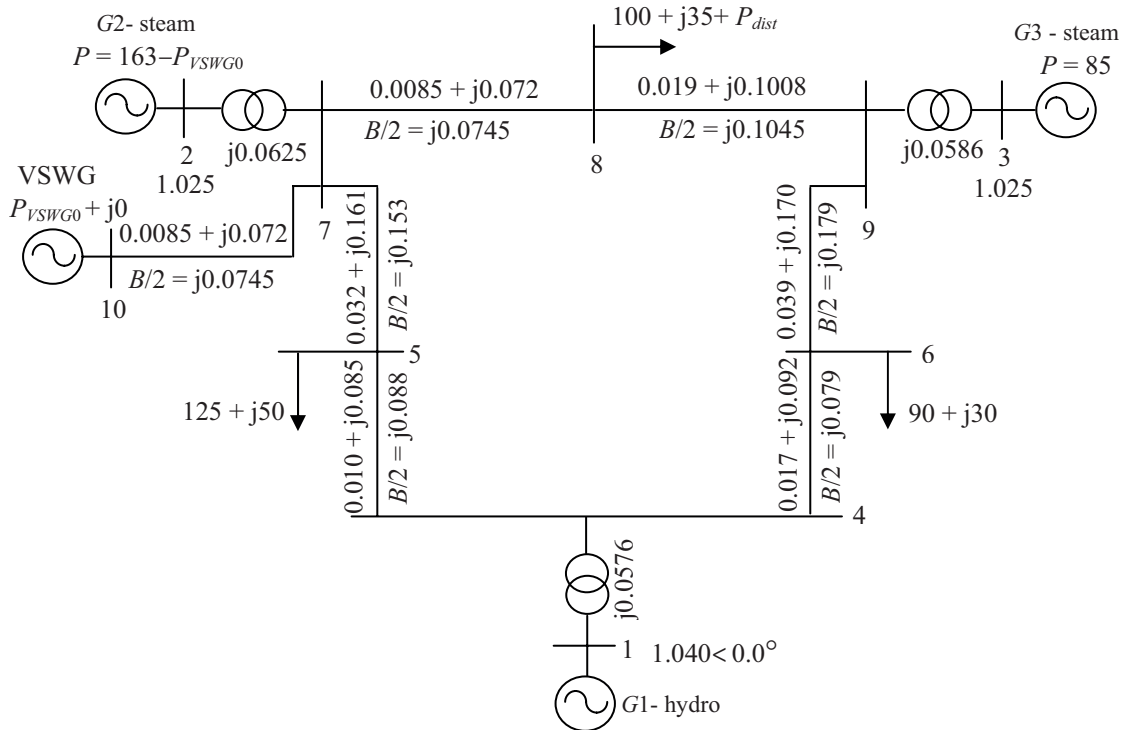


Figure 5. Modified nine-bus system adopted from [21] with included VSWG on bus 10.

**Table 2.** Generator and turbine data adopted from [21] (see Figure 5).

Generator	1	2	3
Rated MVA	247.5	192.0	128.0
Type	Hydro	Steam	Steam
$x_d$	0.1460	0.8958	1.3125
$x'_d$	0.0608	0.1198	0.1813
$H$	23.64	6.40	3.01
$D$ (damping)	2	2	2

Note: reactance values in pu on a 100-MVA base.

**Table 3.** MATLAB Function Block: Hydraulic Turbine and Governor Data.

Servo motor [ $K_a, T_a$ ]	[10/3 0.07]
Gate opening limits [ $g_{min}, g_{max}, vg_{min}, vg_{max}$ ]	[0.01 0.97518 -0.1 0.1]
Permanent drop and regulator [ $R_p, K_p, K_i, K_d, T_d$ ]	[0.05 1.163 0.105 0 0.01]
Hydraulic turbine [ $\beta, T_w$ ]	[0 2.67]
Drop reference (0 = power error, 1 = gate opening)	0

**Table 4.** MATLAB Function Block: Steam Turbine and Governor Data.

Generator type	Tandem-compound (single mass)
Regulator gain, perm. droop, dead zone [ $K_p, R_p, D_z$ ]	[1 0.05 0]
Speed relay and servo motor time constants [ $T_{sr}, T_{sm}$ ]	[ 0.001 0.15]
Gate opening limits [ $vg_{min}, vg_{min}, g_{min}, g_{max}$ ]	[-0.2 0.2 0 6]
Nominal speed of synchronous machine (rpm)	3600
Steam turbine time constants [ $T_2, T_3, T_4, T_5$ ]	[0 0.2 5 0.3]
Turbine torque fractions [ $F_2, F_3, F_4, F_5$ ]	[0 0.3 0.3 0.4]

The simulation is performed using MATLAB and Simulink. The VSWG in the network simulation is presented as  $PQ$  source. Other generators are presented as constant voltage sources. Many EPS are represented as  $PQ$  nodes, where effects of load changes due to frequency variations are modeled with the load-damping constant ( $D$ ) of each generator, excluding the VSWG. Initial load flow calculation is performed using the Newton–Raphson iterative scheme. Dynamic models of all generators, including the VSWG, are realized in Simulink, whereas the power grid is modeled as a MATLAB function. The Runge–Kutta method (ode4) is used as solver type in Simulink. Inputs in the MATLAB function are voltage angles of synchronous generators and active power  $P$  of VSWG ( $Q = 0$ ). Outputs from the MATLAB function file are active and reactive powers of synchronous generators and voltage phasors of the  $PQ$  nodes. In each simulation step, grid response calculations are performed using Newton–Raphson iterative scheme.

After 0.1 s from starting the simulation, active power disturbances (load increase) of different amounts with a maximum value of 50 MW (0.5 pu) are injected into bus 8. The simulation is also performed for varying wind speeds, from 4 m/s to almost 12 m/s. For these wind speeds, the pitch compensator keeps the pitch angle at  $0^\circ$ , ensuring that the extracted mechanical power is maximal. Based on the simulation results, it was found that in the analyzed system from Figure 5, for a disturbance of 50 MW at bus 8, the pitch compensator starts to increase pitch angle when initial wind speed is (approximately) more than 11.5 m/s. In Figure 6, frequency response at bus 7, after an active power disturbance of 30 MW, is shown. The response is shown for 3 different cases: with inertial support control as presented in Figure 3 (modified control algorithm), with inertial support

control as presented in Figure 2, and without inertial support control. The gain of the inertial controller in both cases of inertial support control is adjusted so that the inertial contributions at a wind speed of 11.5 m/s are almost identical. This is the reason why frequency deviations are identical in both cases. From Figure 6 it can be seen that by using inertial support frequency control, both the nadir and the rate of change of frequency are considerably decreased. In Figure 7, the presented injected active powers also show good agreement in both cases of inertial support. Injected active powers in both cases are almost identical; thus, they appear almost as a single line in Figure 7. The maximum injected active power for frequency support is approximately 6.5 MW. From Figure 8 it can be seen that the VSWG speed decrease is less than 2%. From Figures 6 and 8 it can be seen that although the injected electrical power of the VSWG is quite oscillatory, the rotational speed of the VSWG does not show oscillatory behavior. This is an important fact, which shows that inertial support does not cause significant stress on the VSWG mechanical subsystems. This is quite a different property from that of classical steam turbines, where steam turbine speed oscillates in line with oscillations of injected electrical power. However, oscillations in injected electrical power cause structural stress on wind turbines. This fact should be taken into account when designing an inertial control algorithm. Figure 9 presents the frequency response for 3 different wind speeds of 5 m/s, 8 m/s, and 11.5 m/s, with a disturbance of 30 MW. It can be seen that the contribution of the modified control algorithm to frequency stabilization, presented in Figure 3, is not dependent on the initial wind speed. This can also be concluded from Figure 10, where injected power using the same control algorithm is almost independent of initial wind speed. It is qualitatively a new result in comparison to the control algorithm proposed in Figure 2, where inertial support decreases when the initial wind speed decreases. Therefore, using the modified control algorithm means that a VSWG behaves similarly to conventional steam plants with synchronous generators, when the wind speed is between 4 m/s and 12 m/s. Namely, as with classical steam generators, inertial support does not depend on initial mechanical power. In Figure 11, the VSWG speed response during inertial support for 3 different wind speeds is presented. It can be seen that for the chosen disturbance, the VSWG speed does not decrease much, even with a low initial wind speed of 5 m/s.

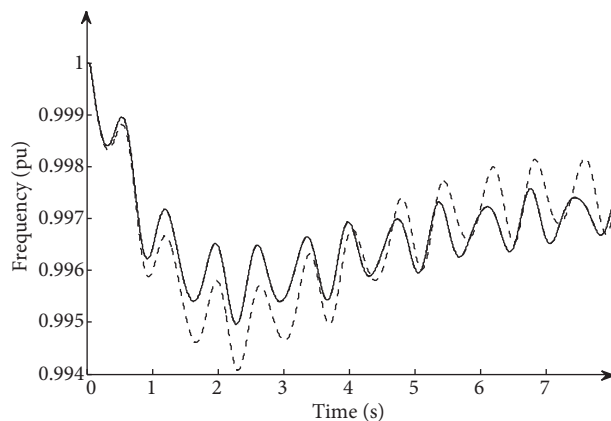


**Figure 6.** Frequency deviation after an active power disturbance of 30 MW (wind speed 11.5 m/s): with inertial supports as in Figures 3 and 2 (solid line); without inertial support (dashed line).

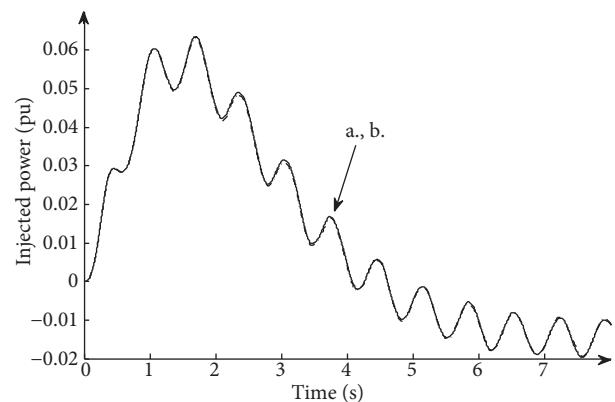


**Figure 7.** Injected power after an active power disturbance of 30 MW (wind speed 11.5 m/s): with inertial support as in Figure 3 (solid line a.) and Figure 2 (dash dotted line b.).

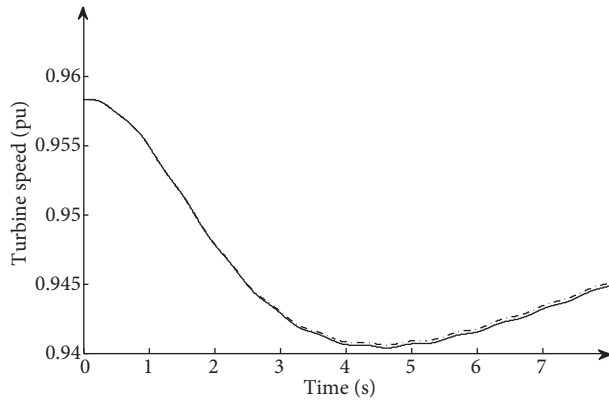


**Figure 8.** VSWG speed after an active power disturbance of 30 MW (wind speed 11.5 m/s): with inertial support as in Figure 3 (solid line) and Figure 2 (dash dotted line).

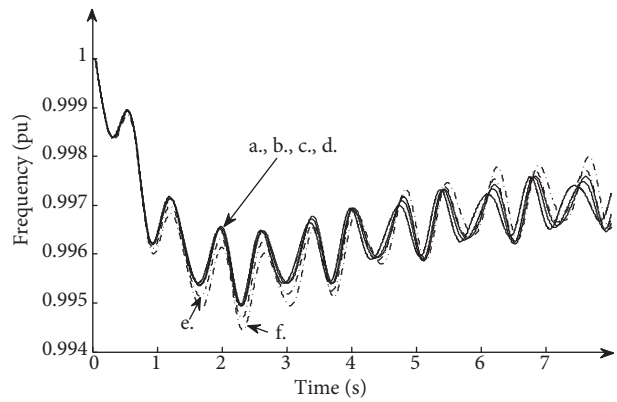


**Figure 9.** Frequency deviation after an active power disturbance of 30 MW: with inertial support as in Figure 3 (solid line for wind speed: a. 11.5 m/s, b. 8 m/s, and c. 3.5 m/s), and with inertial support as in Figure 2 (dash dotted line for wind speed: d. 11.5 m/s, e. 8 m/s, and f. 5 m/s).

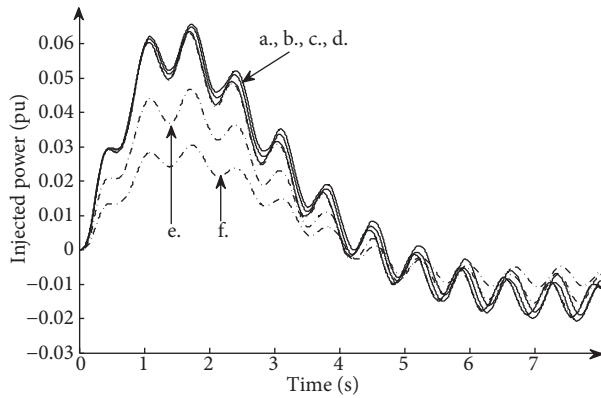


**Figure 10.** Injected power after an active power disturbance of 30 MW: with inertial support as in Figure 3 (solid line for wind speed: a. 11.5 m/s, b. 8 m/s, and c. 3.5 m/s), and with inertial support as in Figure 2 (dash dotted line for wind speed: d. 11.5 m/s, e. 8 m/s, and f. 5 m/s).

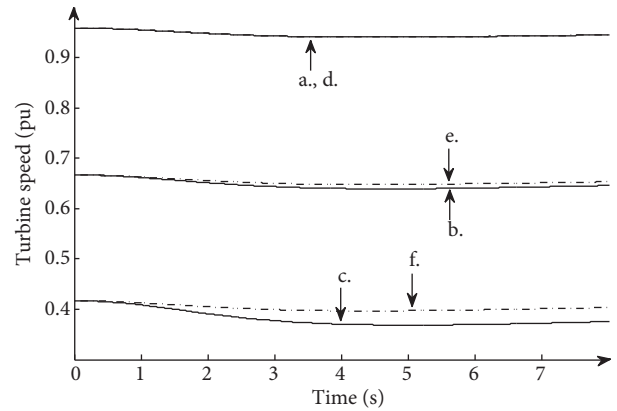


**Figure 11.** The VSWG speed after an active power disturbance of 30 MW: with inertial support as in Figure 3 (solid line for wind speed: a. 11.5 m/s, b. 8 m/s, and c. 5 m/s), and with inertial support as in Figure 2 (dash dotted line for wind speed: d. 11.5 m/s, e. 8 m/s, and f. 5 m/s).

Another important question that should be answered is “What is the maximum expected VSWG speed deviation due to the inertial support?” A contribution to the analysis of this issue is presented below. There is a linear relationship between the optimal turbine speed and wind speed when wind speed is between cut-in and rated speed. Hence:

$$\frac{v_{w1}}{v_{w2}} = \frac{\omega_{t1}}{\omega_{t2}} = k \tag{10}$$

where  $k$  is the constant of proportionality. From Eq. (10), and taking into account that when the modified control algorithm is implemented, the VSWG-injected power during a disturbance is independent of the initial wind speed, it follows that for 2 different wind speeds and for the same disturbance, the following relation is

valid:

$$\frac{1}{2}J\omega_{t1}^2 - \frac{1}{2}J(\omega_{t1} - \Delta\omega_{t1})^2 = \frac{1}{2}J\omega_{t2}^2 - \frac{1}{2}J(\omega_{t2} - \Delta\omega_{t2})^2, \quad (11)$$

where  $\Delta\omega_{t1}$  and  $\Delta\omega_{t2}$  are maximum turbine speed deviations after disturbance with 2 wind speeds,  $v_{w1}$  and  $v_{w2}$ .  $J$  is the moment of inertia of VSWG. From Eq. (11) it follows that:

$$\omega_{t1}\Delta\omega_{t1} - \frac{1}{2}\Delta\omega_{t1}^2 = \omega_{t2}\Delta\omega_{t2} - \frac{1}{2}\Delta\omega_{t2}^2. \quad (12)$$

If a large deviation of turbine speed is not expected (which has been shown by simulations) the squared terms on the left and right hand side of Eq. (12) can be neglected, and then:

$$\omega_{t1}\Delta\omega_{t1} \approx \omega_{t2}\Delta\omega_{t2} \quad (13)$$

or

$$\frac{\Delta\omega_{t1}}{\Delta\omega_{t2}} \approx \frac{\omega_{t2}}{\omega_{t1}} = \frac{1}{k}. \quad (14)$$

It can be concluded that, by using the modified control algorithm, the maximum turbine speed deviation is inversely proportional to the initial wind speed or the initial turbine speed when wind speed is between cut-in and rated wind speed. Table 5 shows the maximum deviations of turbine speed for 3 different wind speeds, based on simulation results that are presented in Figure 11. By using simple calculation it is possible to verify the accuracy of Eq. (14).

**Table 5.** Turbine speed deviation during inertial response for different wind speeds.

Wind speed (m/s)	Turbine speed (pu)	Maximal turbine speed deviation (pu)	Relative turbine speed deviation (%)
5	0.41665	0.04828	11.58853
8	0.66665	0.02740	4.11006
11.5	0.95833	0.01795	1.87283

#### 4. Conclusion

Due to increased ratios of VSWG penetration in electrical energy generation portfolios, the frequency dynamic response of EPS is worsening. In order to reverse this trend, VSWGs should “replace” conventional generating units of EPS, yet not only in stationary state; VSWGs must also contribute to frequency stabilization. Using the modified control algorithm, it is ensured that, in the first seconds after an active power disturbance, the VSWGs “behave” in a similar manner to conventional steam-generating units. Using the modified control algorithm, the VSWG-injected electrical power is independent of the initial steady state (initial wind speed) after a power disturbance, which is characteristic of conventional steam units with synchronous generators. This ensures that the electric power system maintains similar frequency dynamic characteristics regardless of the penetration ratio of the VSWG. From the performed simulations and the results of the analysis, it is shown that turbine speed deviations are not too large for different unbalances, and that the oscillation of the system frequency is not translated into an oscillation of wind turbine speed. Promising areas for future work are the development of more sophisticated control algorithms (including signal processing of the network frequency signal) and the extension of the control strategy to the region of wind speed from 12 m/s to 25 m/s. The nonlinear analysis of the VSWG control system also presents an interesting area for further research.

## References

- [1] Anaya-Lara O, Jenkins N, Ekanayake J, Cartwright P, Hughes M. *Wind Energy Generation: Modelling and Control*. 1st ed. Chichester, UK: Wiley, 2009.
- [2] Yingcheng X, Nengling T. Review of contribution to frequency control through variable speed wind turbine. *Renew Energ* 2011; 36: 1671–1677.
- [3] Ackerman T. *Wind Power in Power Systems*. 2nd ed. Chichester, UK: Wiley, 2012.
- [4] Aho J, Buckspan A, Laks J, Fleming P, Dunne F, Churchfield M, Jeong Y, Pao L, Johnson K. Tutorial of wind turbine control for supporting grid frequency through active power control. In: *American Control Conference 2012; 27–29 June 2012; Montreal, Canada*. New York, NY, USA: IEEE. pp. 3120–3131.
- [5] Hughes FM, Anaya-Lara O, Jenkins N, Strbac G. Control of DFIG-based wind generation for power network support. *IEEE T Power Syst* 2005; 20: 1958–1966.
- [6] Morren J, de Haan SWH, Kling WL, Ferreira JA. Wind turbines emulating inertia and supporting primary frequency control. *IEEE T Power Syst* 2006; 21: 433–434.
- [7] Ramtharan G, Ekanayake JB, Jenkins N. Frequency support from doubly fed induction generator wind turbines. *IET Renew Power Gen* 2007; 1: 3–9.
- [8] Ullah NR, Thiringer T, Karlsson D. Temporary primary frequency control support by variable speed wind turbines—potential and applications. *IEEE T Power Syst* 2008; 23: 601–612.
- [9] Conroy JF, Watson R. Frequency response capability of full converter wind turbine generators in comparison to conventional generation. *IEEE T Power Syst* 2008; 23: 649–656.
- [10] Keung PK, Li L, Banakar H, Ooi BT. Kinetic energy of wind-turbine generators for system frequency support. *IEEE T Power Syst* 2009; 24: 279–287.
- [11] Duval J, Meyer B. Frequency behavior of grid with high penetration rate of wind generation. In: *IEEE 2009 PowerTech 2009 Conference; 28 June–2 July 2009; Bucharest, Romania*. New York, NY, USA: IEEE. pp. 1–6.
- [12] Akbari M, Madani SM. Participation of DFIG based wind turbines in improving short term frequency regulation. In: *ICEE 2010 Electrical Engineering Conference; 11–13 May 2010; Isfahan, Iran*. New York, NY, USA: IEEE. pp. 874–879.
- [13] Mauricio JM, Marano A, Gomez-Exposito A, Ramos JLM. Frequency regulation contribution through variable-speed wind energy conversion systems. *IEEE T Power Syst* 2009; 24: 173–180.
- [14] Gautam D, Goel L, Ayyanar R, Vittal V, Harbour T. Control strategy to mitigate the impact of reduced inertia due to doubly fed induction generators on large power systems. *IEEE T Power Syst* 2011; 26: 214–224.
- [15] Sun YZ, Zhang ZS, Li GJ, Lin J. Review on frequency control of power systems with wind power penetration. In: *POWERCON 2010 International Conference on Power Systems Technology; 24–28 October 2010; Hangzhou, China*. New York, NY, USA: IEEE. pp. 1–8.
- [16] Miller NW, Price WW, Sanchez-Gasca JJ. *Dynamic Modeling of GE 1.5 and 3.6 Wind Turbine-Generators*. Schenectady, NY, USA: GE-Power System Energy Consulting, 2003.
- [17] Miller NW, Sanchez-Gasca JJ, Price WW, Delmerico RW. Dynamic modeling of GE 1.5 and 3.6 MW wind turbine-generators for stability simulations. In: *IEEE 2003 Power Engineering Society General Meeting; 13–17 July 2003; Toronto, Canada*. New York, NY, USA: IEEE. pp. 1977–1983.
- [18] Ellis A, Kazachkov Y, Muljadi E, Pourbeik P, Sanchez-Gasca J. Description and technical specifications for generic WTG models—a status report. In: *IEEE 2011 Power Systems Conference and Exposition; 20–23 March 2011; Phoenix, AZ, USA*. New York, NY, USA: IEEE. pp. 1–8.
- [19] Clark K, Miller NW, Sanchez-Gasca JJ. *Modeling of GE Wind Turbine-Generators for Grid Studies*. Schenectady, NY, USA: General Electric International, 2010.
- [20] Ullah NR. *Wind power: added value for network operations*. PhD, Chalmers University of Technology, Goteborg, Sweden, 2008.
- [21] Anderson PM, Fouad AA. *Power System Control and Stability*. 2nd ed. New York, NY, USA: Wiley, 2003.